Governing failure mode of unsaturated soil slopes under rainwater infiltration

Wengui Huang, Eng-Choon Leong[1,a] and Harianto Rahardjo[1]

[1]*School of Civil & Environmental Engineering, Nanyang Technological University, Singapore*

Abstract. Due to rainwater infiltration and loss of matric suction above the wetting font, both translational and rotational slips may occur in an unsaturated soil slope. It is useful to know which failure mode is more critical. The governing failure mode is likely to be affected by soil properties, slope geometry, depth of wetting front and contribution of matric suction to shear strength, which were investigated in this study. Specifically, upper bound limit analysis was adopted to develop stability charts based on rotational failure mechanism, and infinite slope model was used to develop stability charts based on translational failure mechanism. For a slope, the failure mechanism which gives the lower factor of safety is the governing failure mode. It was found that the failure mode of an unsaturated soil slope under rainfall is determined by parameter group $c'/\gamma H\tan\phi'$ for a given slope angle, depth of wetting front and contribution of matric suction to shear strength. With the increase in depth of wetting front and greater contribution of matric suction to shear strength, a slope is more prone to translational failure. Slopes with angle β = 45º are most vulnerable to translational failure, while gentler slopes (e.g. β = 15º) and steeper slopes (e.g. β = 75º) are more susceptible to rotational failure.

1 Introduction

For an unsaturated soil slope under rainwater infiltration, with the increase in depth of wetting front and the reduction of matric suction above the wetting front, both translational failure and rotational failure may occur, as shown in Figure 1. Most rainfall-induced landslides were reported to be shallow, with a depth of failure less than 3m above the groundwater table [1-2]. Deep-seated landslides after rainfall were also reported [3-4]. Therefore, there are generally two approaches to analyse rainfall-induced landslides. First, the slope is treated as "infinite" with the neglect of boundary effects and infinite slope analysis is performed to assess the slope stability [5-8]. Second, the slope is treated as "finite" with boundary conditions and extended limit equilibrium analysis is performed to assess the slope stability [9-11].

Infinite slope analysis can assess the stability based on translational failure mechanism, but it cannot assess the stability based on rotational failure mechanism. Limit equilibrium analysis can obtain the global factor of safety, but it may fail to search for the potential shallow slip surface [12]. Hence, if only infinite slope analysis or limit equilibrium analysis is performed, alternative failure mechanism may be missed.

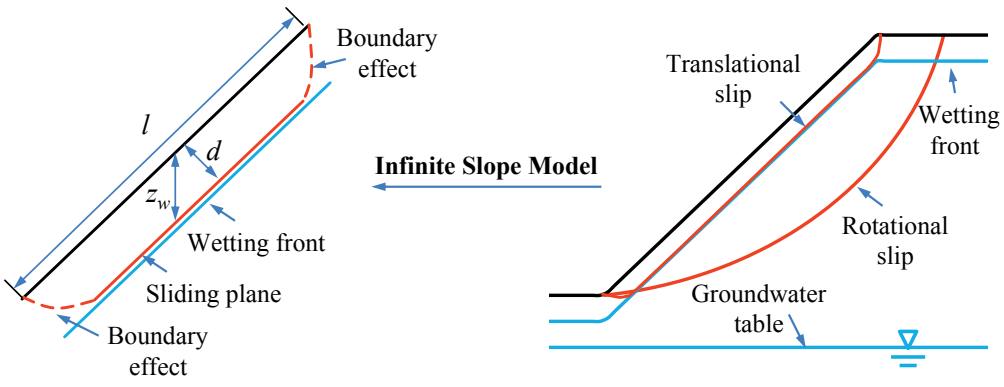

Figure 1. Rotational and translational failures in an unsaturated soil slope

[a] Corresponding author: CECLEONG@ntu.edu.sg

The finite element analysis with a local factor of safety concept [12-13] can detect the potential shallow slip surface if it is more critical than the rotational slip surface. However, it is cumbersome to run a finite element analysis to determine whether a translational or rotational slip is more critical. Hence, the objective of this research is to investigate the controlling factors on the governing failure mode of unsaturated soil slopes under rainfall. The factors investigated include soil properties, slope geometry, depth of wetting front and contribution of matric suction to shear strength. The research will provide guidance in choosing the analysis method for rainfall-induced landslide analysis.

2 Methodology

In order to investigate the governing failure mode of unsaturated soil slopes under rainfall, the stability charts for unsaturated soil slopes under rainwater infiltration based on both translational failure mechanism and rotational failure mechanism were developed. For a slope with specific soil properties, the failure mechanism which gives the lower factor of safety is the governing failure mode of the slope. The stability of an unsaturated soil slope is directly related to the pore-water pressure profile before and after the rainwater infiltration, which will be introduced first. Afterwards, the methodology to develop stability charts based on both rotational failure mechanism and translational failure mechanism will be explained.

2.1 Pore-water pressure profiles

Pore-water pressure profile of an unsaturated soil slope is directly related to the location of the groundwater table and the surface flux condition [14]. Under no infiltration condition, for simplification the matric suction above groundwater table can be treated as hydrostatic relative to the groundwater table. Under rainwater infiltration, as shown in Figure 2, the matric suction can be partially lost (profile a), completely lost (profile b), or positive pore-water pressure may even build up above the wetting front (profile c) [15].

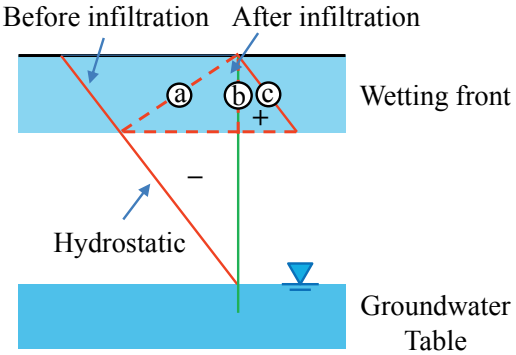

Figure 2. Pore-water pressure profiles before and after infiltration (modified from [15])

Research shows that profile a tends to occur in fine-grained soils, profile b tends to occur in coarse-grained soils [7] and profile c tends to occur in layered soils with permeable layer above wetting front and less permeable layer below wetting front [8]. In this research, profile c is not considered, as the research focuses on slopes made of homogeneous soils. The pore-water pressure profile b is adopted, which is a reasonable assumption for coarse-grained soils and a conservative assumption for fine-grained soils.

2.2 Stability chart based on rotational failure mechanism

Upper bound limit analysis has been widely used to develop stability charts for simple homogeneous soil slopes [16-17] and soil slopes under positive pore-water pressures [18-19]. Recently Huang et al. [20] incorporated negative pore-water pressure into the upper bound limit analysis and developed stability charts for unsaturated soil slopes under no infiltration condition. The research can be further extended by considering the depth of wetting front and stability charts for unsaturated soil slopes under infiltration condition can be developed subsequently.

According to the upper bound limit analysis, soil mass would fail if the rate of work done by soil weight and external forces exceeds the internal rate of energy dissipation. Hence, equating the external rate of work to the internal rate of energy dissipation gives an unsafe upper bound on the collapse or limit load [17].

For a simple homogeneous slope, the energy balance equation can be written as:

$$\dot{W}_{\gamma} = \dot{D}_{c'} \tag{1}$$

where $\dot{W}_{\gamma}$ is the rate of work done by soil weight, $\dot{D}_{c'}$ is the rate of internal energy dissipation.

If pore-water pressure is incorporated into the upper bound limit analysis and treated as external force, the energy balance equation can be expressed as (e.g., [21]):

$$\dot{W}_{\gamma} + \dot{W}_{u} = \dot{D}_{c'} \tag{2}$$

where $\dot{W}_{u}$ is the rate of work done by pore-water pressure u_w.

In the upper bound limit analysis, plastic shearing is assumed to follow associated flow rule, which requires that the velocity jump vector at slip surface is inclined to the slip surface at the effective angle of internal friction ϕ'. Hence, for a rotational failure, the slip surface must be a log-spiral curve [17, 21], as described by Equation (3) and shown in Figure 3, in which r_o is initial radius of the log-spiral curve, θ_o and θ_h are initial and final angles, $r(\theta)$ is the radius which is a function of θ. In Figure 3, H is the height of the slope, L is the length of the slope at the crest, α is the slope angle at the crest, β is the slope angle at the toe. If the slip surface passes below the toe (base failure), the inclination angle from the crest point (B) of the slope to the end point of the slip surface (C′) is β', and $\beta' = \beta$ if the slip surface passes through the toe (toe failure).

$$r(\theta) = r_o \exp[(\theta - \theta_o)\tan\phi'] \quad (3)$$

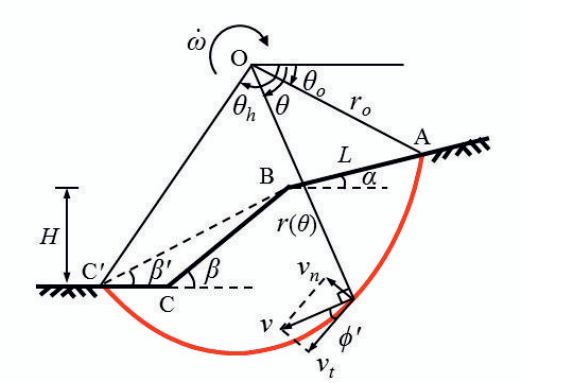

Figure 3. Log-spiral rotational failure

For rotational failure, $\dot{W}_\gamma$ can be calculated by a direct integration of the dot product of the unit weight vector $\boldsymbol{\gamma}$ and the velocity vector $\mathbf{v}$ over the region A - C' - C - B:

$$\dot{W}_\gamma = \int_V \boldsymbol{\gamma} \bullet \mathbf{v} \mathrm{d}V = \dot{\omega}\gamma r_o^3 (f_1 - f_2 - f_3 - f_4) \quad (4)$$

where $\dot{\omega}$ is the rate of rotation of the failed mass around the centre O, as shown in Figure 3. Coefficients f_1 to f_4 depend on the given values of α, β and ϕ', and variables θ_o, θ_h and β', and have been given by Chen [17].

$\dot{D}_{c'}$ can be calculated by the integration of the product of effective cohesion c' and tangential component of velocity v_t over the slip surface S:

$$\dot{D}_{c'} = \int_S c' v_t \mathrm{d}S = \frac{c'\dot{\omega}r_o^2}{2\tan\phi'}\{\exp[2(\theta_h - \theta_o)\tan\phi'] - 1\} \quad (5)$$

For a rigid rotation, the rate of work done by positive pore-water pressure can be calculated by [21]:

$$\dot{W}_u = \int u_w \tan\phi' \dot{\omega} r^2(\theta)\mathrm{d}\theta \quad (u_w \geq 0) \quad (6)$$

The rate of work done by negative pore-water pressure can be calculated by [20]:

$$\dot{W}_u = \int u_w \tan\phi^b \dot{\omega} r^2(\theta)\mathrm{d}\theta \quad (u_w < 0) \quad (7)$$

where ϕ^b is the rate of increase of shear strength due to matric suction.

Figure 4 shows the geometry of an unsaturated soil slope. The groundwater table is defined as a straight line [10, 11, 20], with a vertical distance H_{wt} between the toe of slope and groundwater table and an inclination angle i. The pore-water pressure u_w is assumed to be hydrostatic relative to the groundwater table before infiltration. After infiltration, the wetting front is assumed to be parallel to the ground surface with a vertical depth z_w, and $u_w = 0$ (profile b) for the soils above the wetting front.

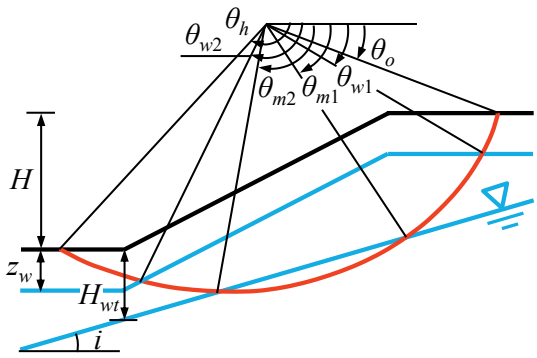

Figure 4. Geometry of an unsaturated soil slope under rainwater infiltration

The rate of work done by pore-water pressure u_w after infiltration can be calculated by:

$$\dot{W}_u = \int_{\theta_{w1}}^{\theta_{m1}} u_w(\theta)\tan\phi^b \dot{\omega} r^2(\theta)\mathrm{d}\theta + \int_{\theta_{m1}}^{\theta_{m2}} u_w(\theta)\tan\phi' \dot{\omega} r^2(\theta)\mathrm{d}\theta + \int_{\theta_{m2}}^{\theta_{w2}} u_w(\theta)\tan\phi^b \dot{\omega} r^2(\theta)\mathrm{d}\theta \quad (8)$$

where θ_{w1} and θ_{w2} are the angles correspond to the intersection points between wetting front and slip surface, θ_{m1} and θ_{m2} are the angles correspond to the intersection points between groundwater table and slip surface, as shown in Figure 4.

If ϕ^b is assumed to be a constant, $\dot{W}_u$ can finally be expressed as:

$$\dot{W}_u = \dot{\omega}\gamma r_o^3 f_{u_w} \quad (9)$$

where f_{u_w} depends on given values of α, β, i, γ_w/γ, H_{wt}/H, z_w/H, ϕ^b and ϕ', and variables θ_o, θ_h and β'. The detailed derivation of f_{u_w} can be found in Huang et al. [20].

Consequently, Equation (2) can be written as:

$$\frac{\gamma H}{c'} = \frac{H}{r_o}\frac{\exp[2(\theta_h - \theta_o)\tan\phi'] - 1}{2\tan\phi'(f_1 - f_2 - f_3 - f_4 + f_{u_w})} \quad (10)$$

In upper bound limit analysis, the soil is assumed to obey the Mohr-Coulomb failure criterion, and factor of safety F is defined as:

$$F = \frac{c'}{c_d} = \frac{\tan\phi'}{\tan\phi_d} \quad (11)$$

in which c_d and ϕ_d are the effective cohesion and effective internal friction angle, respectively, that are necessary to maintain energy balance in an admissible failure mechanism.

In order to present the stability charts as dimensionless forms, among the given conditions, i is normalized with β as i/β, and ϕ^b is normalized with ϕ' as ϕ^b/ϕ'. Furthermore, it is fixed that $\alpha = 0°$ and $\gamma_w/\gamma = 0.5$ for all the stability charts developed in this study. For a given slope angle β and ratios of H_{wt}/H, i/β, z_w/H, and ϕ^b/ϕ', the minimum value of $\gamma H/c'$ in Equation (10) can be

found for a given value of ϕ' with θ_o, θ_h and β' being the variables. The obtained minimum $\gamma H/c'$ and corresponding ϕ' are denoted as $\gamma H/c_d$ and ϕ_d, respectively. Stability charts can be presented as $c_d/\gamma H$ being a function of ϕ_d (e.g. [22-24]). However, since F must be applied to both c' and $\tan\phi'$ [see Equation (11)], tedious iterations are required to obtain F from such charts [18, 24].

With the obtained $\gamma H/c_d$ and ϕ_d, Equation (10) can be rewritten as:

$$\frac{1}{\tan\phi_d} = \frac{2(\theta_h - \theta_o)}{\ln\left[1 + 2\frac{\gamma H \tan\phi_d}{c_d}\frac{r_o}{H}\left(f_1 - f_2 - f_3 - f_4 + f_{u_w}\right)\right]} \quad (12)$$

Parameter group $c'/\gamma H\tan\phi'$ is dimensionless and independent of F [25]:

$$\frac{c_d}{\gamma H \tan\phi_d} = \frac{c'/F}{\gamma H \tan\phi'/F} = \frac{c'}{\gamma H \tan\phi'} \quad (13)$$

According to Equations (11) and (13), Equation (12) can be rearranged to be:

$$\frac{F}{\tan\phi'} = \frac{2(\theta_h - \theta_o)}{\ln\left[1 + 2\frac{\gamma H \tan\phi'}{c'}\frac{r_o}{H}\left(f_1 - f_2 - f_3 - f_4 + f_{u_w}\right)\right]} \quad (14)$$

Stability charts can be developed by setting $F/\tan\phi'$ as a function of $c'/\gamma H\tan\phi'$ (e.g. [18-20]). The advantage of this format is that factor of safety of a slope can be obtained without iteration [18].

2.3 Stability chart based on translational failure mechanism

Factor of safety of a slope based on translational failure mechanism can be obtained by performing infinite slope analysis with the neglect of boundary effects. For a translational slip with pore-water pressure profile b (Figure 2) above wetting front and by using infinite slope model, F can be calculated as [15]:

$$F = \frac{c'}{\gamma z_w \sin\beta\cos\beta} + \frac{\tan\phi'}{\tan\beta} \quad (15)$$

Equation (15) can be rearranged to be:

$$\frac{F}{\tan\phi'} = \frac{c'}{\gamma H \tan\phi'}\frac{H}{z_w}\frac{1}{\sin\beta\cos\beta} + \frac{1}{\tan\beta} \quad (16)$$

Hence, for given z_w/H and β, stability chart based on translational failure mechanism can also be presented by setting $F/\tan\phi'$ as a function of $c'/\gamma H\tan\phi'$. However, it should be noted that infinite slope model would underestimate the factor of safety due to the neglect of boundary effects, and the accuracy of infinite slope analysis is directly related to the depth/length ratio of the translational slip [26-27].

3 Results and discussions

Figure 5 shows an example of the developed stability charts. The solid curve is developed based on translational failure mechanism with the condition that β = 45º and z_w/H = 0.1, the dash curve is developed based on rotational failure mechanism with the condition that β = 45º, z_w/H = 0.1, H_{wt}/H = 0.2, i = 0° and ϕ^b/ϕ' = 1/3. It is shown that there is an intersection point between the stability curves. The corresponding $c'/\gamma H\tan\phi'$ at the intersection point is defined as critical $c'/\gamma H\tan\phi'$. Below this critical value the translational failure mechanism would give a lower factor of safety and govern the failure mode. Above this critical value the rotational failure mechanism would give a lower factor of safety and govern the failure mode. For a slope, the higher the critical $c'/\gamma H\tan\phi'$, the more vulnerable the slope is to translational failure.

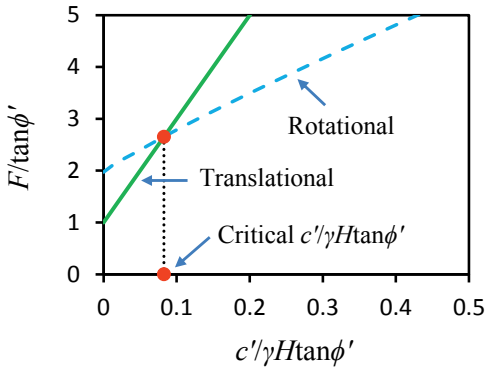

Figure 5. Stability charts for rotational failure and translational failure

A parametric study has been carried out to investigate the influence of slope angle (β), depth of wetting front (z_w/H), and contribution of matric suction (ϕ^b/ϕ', H_{wt}/H and i/β) on the critical $c'/\gamma H\tan\phi'$. The adopted parameters are shown in Table 1.

Table 1. Parametric study to the critical $c'/\gamma H\tan\phi'$

β =	15º, 30º, 45º, 60º, 75º
z_w/H =	0.05, 0.10, 0.15, 0.20
ϕ^b/ϕ' =	0, 1/3, 2/3, 1
H_{wt}/H =	0.2
i/β =	0

A typical plot indicating the influence of z_w/H on the critical $c'/\gamma H\tan\phi'$ is shown in Figure 6. It is found that the critical $c'/\gamma H\tan\phi'$ increases with the increase in z_w/H, and the curves are concave upward. The results reveal that with the increase in depth of wetting front, the slope becomes more prone to translational failure.

A typical plot representing the influence of ϕ^b/ϕ' on critical $c'/\gamma H\tan\phi'$ is shown in Figure 7. It is shown that the critical $c'/\gamma H\tan\phi'$ increases with the increase in ϕ^b/ϕ', but the curves are concave downward. The results reveal that due to the greater contribution of matric suction to shear strength, the slope becomes more susceptible to translational failure.

A typical plot showing the influence of β on critical $c'/\gamma H\tan\phi'$ is illustrated in Figure 8. It is shown that the

critical $c'/\gamma H\tan\phi'$ obtains its peak value at $\beta = 45°$, and it decreases with both the increase and decrease of β. The results reveal that slopes with angle $\beta = 45°$ are most vulnerable to translational failure, while gentler slopes (e.g. $\beta = 15°$) and steeper slopes (e.g. $\beta = 75°$) are more disposed to rotational failure.

However, it should be reminded that the stability chart for translational failure mechanism is developed based on the infinite slope model, which neglects boundary effects and the obtained factors of safety are underestimated. Hence, the critical $c'/\gamma H\tan\phi'$ shown from Figures 5 to 8 may be slightly overestimated.

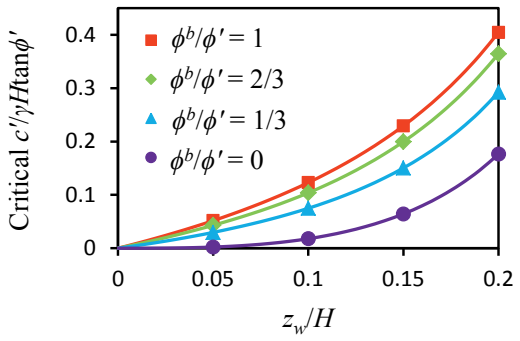

Figure 6. Influence of z_w/H on critical $c'/\gamma H\tan\phi'$ ($\beta = 30°$)

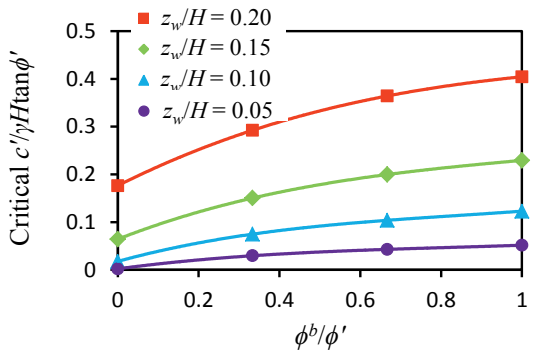

Figure 7. Influence of ϕ^b/ϕ' on critical $c'/\gamma H\tan\phi'$ ($\beta = 30°$)

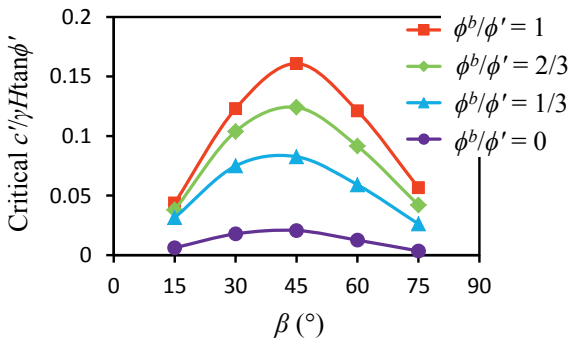

Figure 8. Influence of β on critical $c'/\gamma H\tan\phi'$ ($z_w/H = 0.10$)

4 Conclusions

For an unsaturated soil slope under rainwater infiltration, the increase in depth of wetting front and the reduction in matric suction above the wetting front may result in either translational or rotational failure mechanism. It is useful to know which failure mode is more critical for a specific slope. The governing failure mode is likely to be affected by soil properties, slope geometry, depth of wetting front and contribution of matric suction to shear strength, which were investigated in this study. Specifically, upper bound limit analysis was adopted to develop stability charts for unsaturated soil slopes under rainwater infiltration based on rotational failure mechanism, and infinite slope model was used to develop stability charts based on translational failure mechanism. The failure mechanism which gives the lower factor of safety is the governing failure mode.

The governing failure mode was found to be determined by the parameter group $c'/\gamma H\tan\phi'$. In addition, a critical $c'/\gamma H\tan\phi'$ exists below which translational failure governs and above which rotational failure governs. The influences of slope angle, depth of wetting front and contribution of matric suction to shear strength on the governing failure mode were preliminary investigated by a parametric study. It was found that with the increase in depth of wetting front and greater contribution of matric suction to shear strength, critical $c'/\gamma H\tan\phi'$ increases and slopes are more prone to translational failure under rainwater infiltration. Slopes with angle $\beta = 45°$ have the highest critical $c'/\gamma H\tan\phi'$ and are most vulnerable to the translational failure, while gentler slopes (e.g. $\beta = 15°$) and steeper slopes (e.g. $\beta = 75°$) are more susceptible to the rotational failure. For the situation when translational failure has more possibility, infinite slope analysis is more preferable to assess the slope stability; otherwise limit equilibrium analysis is more desirable to assess the slope stability.

Acknowledgement

The first author gratefully acknowledges the research scholarship provided by Nanyang Technological University (Singapore).

References

1. F.C. Dai, C.F. Lee, S.J. Wang, Int. J. Remote Sens., **24**(23), 4817-4834 (2003)
2. K.A. Johnson, N. Sitar, Can. Geotech. J., **27**(6), 789-801 (1990)
3. D.M.S. Gerscovich, E.A. Vargas, T.M.P. De Campos, Eng. Geol., **88**(1), 23-40 (2006)
4. B.B. Huat, F.H. Ali, R.S.K. Rajoo, Am. J. Environ. Sci., **2**(4), 154-160 (2006)
5. D. Pradel, G. Raad, J. Geotech. Eng., **119**(2), 315-332 (1993)
6. B.D. Collins, D. Znidarcic, J. Geotech. Geoenviron. Eng., **130**(4), 362-372 (2004)
7. L.M. Lee, N. Gofar, H. Rahardjo, Eng. Geol., **108**(3), 272-285 (2009)
8. S.E. Cho, Eng. Geol., **105**(1), 32-43 (2009)
9. I. Tsaparas, H. Rahardjo, D.G. Toll, E.C. Leong, Comput. Geotech., **29**(1), 1-27 (2002)
10. H. Rahardjo, T.H. Ong, R.B. Rezaur, E.C. Leong, J. Geotech. Geoenviron. Eng., **133**(12), 1532-1543 (2007)
11. A. Rahimi, H. Rahardjo, E.C. Leong, J. Geotech. Geoenviron. Eng., **137**(5), 483–491 (2011)

12. N. Lu, B. Şener-Kaya, A. Wayllace, J.W. Godt, Water Resour. Res., **48**(9) (2012)
13. E.E. Alonso, A. Gens, C.H. Delahaye, Hydrogeol. J., **11**(1), 174-192 (2003)
14. D.G. Fredlund, H. Rahardjo, *Soil mechanics for unsaturated soils*, John Wiley & Sons (1993)
15. H. Rahardjo, T.T. Lim, M.F. Chang, D.G. Fredlund, Can. Geotech. J., **32**(1), 60-77 (1995)
16. W.F. Chen, M.W. Giger, H.Y. Fang, Soils Found., **9**(4), 23-32 (1969)
17. W.F. Chen, *Limit analysis and soil plasticity*, Elsevier Science, Amsterdam, the Netherlands (1975)
18. R.L. Michalowski, J. Geotech. Geoenviron. Eng., **128**(4), 351-355 (2002)
19. R.L. Michalowski, S. Nadukuru, J. Geotech. Geoenviron. Eng., **139**(9), 1604-1610 (2013)
20. W. Huang, E.C. Leong, H. Rahardjo, J. Geotech. Geoenviron. Eng. (submitted)
21. R.L. Michalowski, Geotechnique, **45**(2), 283-293 (1995)
22. D.W. Taylor, J. Boston Soc. Civil Eng., **24**(3), 197-246 (1937)
23. A.W. Bishop, N. Morgenstern, Geotechnique, **10**(4), 129-153 (1960)
24. E. Spencer, Geotechnique, **17**(1), 11-26 (1967)
25. J.M. Bell, J. Soil Mech. and Found. Div., **92**(5), 51-65 (1966)
26. D.V. Griffiths, J. Huang, G.F. Dewolfe, Int. J. Numer. Anal. Met. Geomech., **35**(5), 569-585 (2011)
27. W. Huang, E. C. Leong, H. Rahardjo, *Unsaturated Soils: Research & Applications*, *Proceedings of the sixth Asia-Pacific conference on unsaturated soils*, *China*, 771-775 (2015)